photonics

MDPI

Article

Sub-40 fs Pulses from a Tapered Yb-Doped Fiber Amplifier with Self-Similar Amplification

Yaqi Wu [1], Bowen Liu [1,2,*], Genyu Bi [1] and Minglie Hu [1,2,*]

[1] Ultrafast Laser Laboratory, State Key Laboratory of Precision Measuring Technology and Instruments, School of Precision Instruments and Opto-Electronics Engineering, Tianjin University, Tianjin 300072, China; yqwu@tju.edu.cn (Y.W.); bigenyu@tju.edu.cn (G.B.)
[2] Georgia Tech Shenzhen Institute, Tianjin University, Shenzhen 518071, China
* Correspondence: bwliu@tju.edu.cn (B.L.); huminglie@tju.edu.cn (M.H.)

Abstract

We extended self-similar amplification to a large-mode-area tapered Yb-doped fiber (LMA T-YDF) with longitudinally decreasing nonlinearity. The theoretical analysis and numerical simulation demonstrate that T-YDFs with different nonlinearity profiles can achieve self-similar evolution, which is confirmed by a self-similar amplifier that employs two kinds of T-YDFs. Further experimental study indicates that the T-YDF with a large core diameter at the thin end can achieve self-similar evolution across a wide range of pump powers and generate 51 W average power, 34 fs nearly transform-limited (TL) pulses with 32 dB gain. To the best of our knowledge, this is the first theoretical and experimental demonstration of self-similar amplification in T-YDFs. The high-gain feature of the T-YDF simplifies the laser system and can be used to build a compact all-fiber high-power femtosecond laser source.

Keywords: fiber amplifiers; self-similar amplification; tapered fiber

1. Introduction

Femtosecond fiber lasers are highly demanded for industrial applications and scientific research owing to their outstanding reliability and compactness [1,2]. Particularly for multi-photon imaging and ultrafast spectroscopy, fiber lasers with high repetition frequency and sub-100 fs pulse duration are preferred [3,4]. Yb-doped fibers are widely used due to their high quantum efficiency, low thermal effects, and high gain compared to other doped fibers. However, the gain bandwidth limits the output spectrum, so the compressed pulse duration is usually >200 fs [5,6]. Still, nonlinear effects, such as self-phase modulation (SPM), can overcome gain narrowing and even broaden the spectrum to tens of nanometers, supporting sub-100 fs pulse durations. This is the main advantage of nonlinear amplification technology, which includes pre-chirp managed amplification, gain-managed nonlinear (GMN) amplification and self-similar amplification (SSA) [7–10]. Among these approaches, SSA uniquely achieves nearly transform-limited (TL) pulses.

SSA utilizes the interplay among SPM, gain, and positive group velocity dispersion (GVD) in long gain fibers to produce linearly chirped parabolic pulses [10]. The output pulses with a linear chirp and broadened spectrum from self-similar amplifiers can be easily dechirped to TL pulses that are shorter than the input pulses. However, the gain bandwidth influences spectrum broadening and distorts self-similar evolution, so long low-gain fibers are typically used to avoid the gain-shaping effect [11]. High-quality 48 fs pulses with 18 W average power in a 6 m gain fiber were achieved [12]. But stimulated

Check for updates

Received: 6 March 2026
Revised: 11 April 2026
Accepted: 6 May 2026
Published: 8 May 2026

Copyright: © 2026 by the authors. Licensee MDPI, Basel, Switzerland. This article is an open access article distributed under the terms and conditions of the Creative Commons Attribution (CC BY) license.

Raman scattering always occurs in long fibers, which also distorts the self-similar evolution and limits the pulse energy [13]. Fortunately, the input pulses can quickly converge to the self-similar regime in a short gain fiber with the proper initial chirp. This approach enabled the generation of sub-40 fs pulses with 80 W average power [14]. Further, by pre-compensating the third-order dispersion, 33 fs pulses with 93.5 W average power were generated [15].

Normally, gain fibers with constant core diameters are used in self-similar amplifiers. SSA has not been demonstrated in an Yb-doped fiber with varying core diameters. Recently, large-mode-area tapered Yb-doped fibers (LMA T-YDFs) whose core diameters increase along the longitudinal direction have been developing rapidly [16–19]. Their length is several meters and the core diameter is far larger than the operating wavelength, which is different from the conventional passive tapered fiber. To produce T-YDFs, the flow rate of inert gas passing through the heating furnace during the drawing process must be altered [20]. The large core diameter of the wide end can help improve the nonlinear threshold and the small core diameter of the thin end can help excite the fundamental mode. The increasing diameter along the direction of the signal propagation results in single-mode operation without bend sensitivity. A compact picosecond T-YDF amplifier with 457 W average power, 38.5 dB gain and near diffraction-limited beam quality was demonstrated [21]. Although the T-YDF has been used as the main amplifier to output femtosecond pulses, pulse durations are >200 fs in high-energy systems [19,22]. Further, a GMN T-YDF amplifier was demonstrated to output 49 fs pulses with 0.58 μJ energy, but the pulses had obvious pedestals and were not TL pulses [23]. It is necessary to improve the pulse quality of the T-YDF amplifier while achieving a short pulse duration. Thus, the T-YDF not only provides a platform to explore whether a gain fiber with a nonuniform longitudinal geometry can achieve SSA, but can also improve the system performance by relying on the advantages of T-YDFs and SSA.

In this paper, we extend SSA to the T-YDF with longitudinally decreasing nonlinearity. Theoretical analysis indicates the pulse evolution in T-YDFs is similar to the evolution in uniform fibers with an equivalent gain, indicating that pulses can also evolve into linearly chirped parabolic pulses in T-YDFs, which is confirmed by the simulation results. To further verify the theoretical and numerical results, we built a self-similar amplifier using two kinds of T-YDFs with different nonlinearity profiles. The results demonstrate they can both achieve SSA, and the T-YDF with a large core diameter at the thin end can achieve self-similar evolution across a wide range of pump powers. Further, we find that a proper negative initial chirp can help obtain nearly TL dechirped pulses, and the optimal initial chirp value decreases as the output power increases. Finally, the system output 34 fs high-quality pulses with 51 W average power and 32 dB gain. To the best of our knowledge, this is the first theoretical and experimental demonstration of SSA in T-YDFs. The high-gain feature of the T-YDF simplifies the laser system and can be used to build a compact all-fiber high-power femtosecond laser source.

2. Theoretical Analysis

Pulse propagation in a T-YDF amplifier can be simply described by the nonlinear Schrödinger equation (NLSE) with a constant gain, neglecting high-order dispersion and high-order nonlinear effects:

$$i\frac{\partial \Psi}{\partial z} = \frac{\beta_2}{2}\frac{\partial^2 \Psi}{\partial T^2} - \gamma(z)|\Psi|^2\Psi + i\frac{g_0}{2}\Psi \quad (1)$$

where $\Psi(z,T)$ is the amplitude of the pulse envelope, β_2 is the second-order dispersion, γ is the nonlinearity parameter, and g_0 is the gain.

Generally, pulses are incident from the thin end of a T-YDF for realizing single-mode operation and a high nonlinear threshold, so nonlinearity is decreasing along the fiber. Further, the core diameter of a T-YDF is significantly larger than the wavelength, so the waveguide dispersion contributes little to β_2, and β_2 can be regarded as a constant. Thus, only the nonlinearity parameter changes along the fiber.

Equation (1) can be transformed into the following form:

$$i\frac{\partial u}{\partial z} - \frac{\beta_2}{2}\frac{\partial^2 u}{\partial T^2} + \gamma(0)|u|^2 u = i\left(\frac{1}{2R}\frac{dR}{dz} + \frac{g_0}{2}\right)u = i\frac{(g_1 + g_0)}{2}u = i\frac{g}{2}u \tag{2}$$

with u, γ, R defined by

$$u(z,T) = \Psi\sqrt{R},\ R(z) = \frac{\gamma(z)}{\gamma(0)},\ g_1(z) = \frac{1}{R}\frac{dR}{dz},\ g = g_1 + g_0 \tag{3}$$

When R is an exponential-type function, like $e^{g_1 z}$, Equation (2) becomes an NLSE with constant gain, which has previously been demonstrated to have an exact asymptotic solution corresponding to linearly chirped parabolic pulses [10]. Therefore, the T-YDF with an exponentially decreasing nonlinearity profile ($g_1 < 0$ and $g > 0$) can also achieve self-similar evolution, and the solution is

$$\Psi(z,t) = \begin{cases} \sqrt{P(z)}\left\{1 - \left[\frac{T}{T_P(z)}\right]^2\right\}^{1/2} \exp[i\varphi(z,t)], & |T| \le T_P(z) \\ 0, & |T| > T_P(z) \end{cases} \tag{4}$$

$$P(z) = \frac{1}{4}\left[\frac{2g^2 {E_0}^2}{\gamma(0)\beta_2}\right]^{1/3} \exp\left(\frac{1}{3}(2g_0 - g_1)z\right) \tag{5}$$

$$T_P(z) = 3\left[\frac{\gamma(0)\beta_2 E_0}{2g^2}\right]^{1/3} \exp\left(\frac{1}{3}gz\right) \tag{6}$$

$$\varphi(z,t) = \varphi_0 + \frac{3}{8}\left(\frac{2\gamma(0)^2 {E_0}^2}{g\beta_2}\right)^{1/3} \exp\left(\frac{2}{3}gz\right) - \frac{g}{6\beta_2}T^2 \tag{7}$$

where E_0 is the input energy.

3. Numerical Simulation

To confirm the analytical solution, the split-step Fourier method is used to conduct the numerical simulation of Equation (1). In the simulation, 0.1 nJ, 400 fs Gaussian pulses are amplified by a 5 m T-YDF, whose core diameters are 10 μm and 50 μm, respectively, on the thin and wide ends, with $\beta_2 = 0.023\ \mathrm{ps^2/m}$, $n_2 = 2.6 \times 10^{-20}\ \mathrm{m^2/W}$ and $g_0 = 1.4\ \mathrm{m^{-1}}$. Further, the nonlinearity parameter is exponentially decreasing along the fiber (Figure 1a). Figure 1b shows temporal profiles of output pulses by the simulation and the theoretical prediction; they are almost identical, and this confirms the analytical model. Moreover, the dechirped pulses are close to the TL pulses (Figure 1c), indicating the output pulses have a linear chirp.

However, the design of the core diameter profiles of T-YDFs needs to consider modal loss, modal power evolution and heat load density [24]. Thus, an exponential nonlinearity profile may not be available, and Equation (2) becomes an NLSE with varying gain which was also demonstrated to have an exact self-similar solution under the limit of high power [25]. But the solution is difficult to analytically calculate for an arbitrary gain profile. Thus, numerical simulations are conducted for non-exponential nonlinearity profiles.

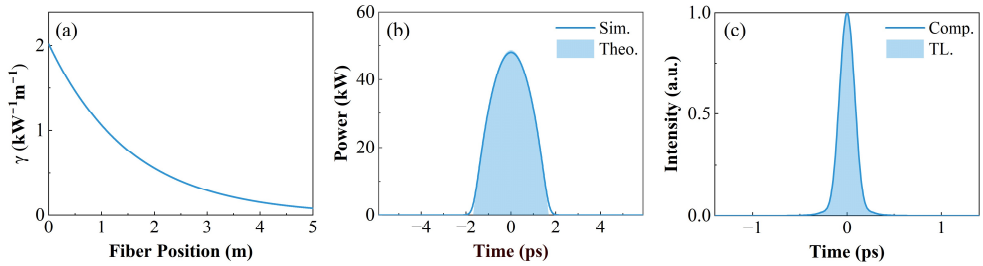

Figure 1. (**a**) The nonlinearity profiles of a T-YDF with exponentially decreasing nonlinearity. (**b**) Temporal profiles of output pulses by simulations (solid line) and the theoretical prediction (shaded area). (**c**) Temporal profiles of dechirped pulses (solid line) and corresponding TL pulses (shaded area).

The nonlinearity profile can be represented by

$$\gamma(z) = \frac{b_0 - b}{L} z^2 + bz + \gamma_1 \tag{8}$$

where γ_1 and γ_2 are the nonlinearity parameters of the thin and wide ends, $b_0 = (\gamma_2 - \gamma_1)/L$ is the average taper angle and b is the parabolic shape factor [26]. According to the relative values of b and b_0, the nonlinearity profile can be divided into convex, linear and concave shapes, as shown in Figure 2a. And other complex profiles can be approximated by these three shapes.

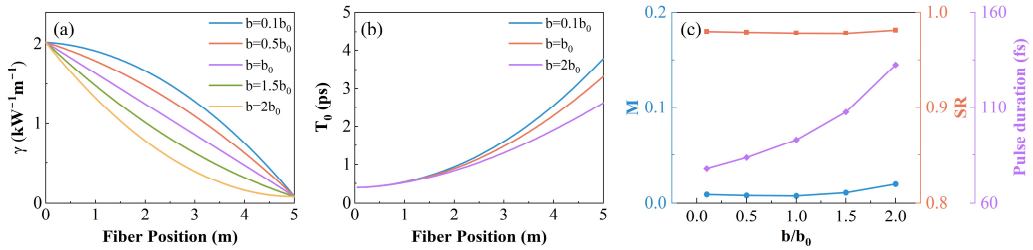

Figure 2. (**a**) The different nonlinearity profiles of T-YDFs. (**b**) Evolution of the pulse duration along the fiber under different nonlinearity profiles. (**c**) M factors, SRs and compressed pulse durations under different nonlinearity profiles.

To judge whether self-similar evolution is achieved, the parameter M is employed to represent the approximate degree of intensity profiles between the output pulse A and a parabolic pulse A_p, calculated by

$$M^2 = \frac{\int \left(|A|^2 - |A_p|^2 \right)^2 dt}{\int |A|^4 dt} \tag{9}$$

SSA is believed to be achieved when M < 0.04 [27]. Moreover, the characteristic of linear chirp is judged by the Strehl ratio (SR), which is the ratio of the peak power of the compressed pulses to that of the TL pulses [28]. When the SR approaches 1, the output pulses have a nearly linear chirp and pulse quality is high.

Figure 2b shows evolutions of the pulse duration along the fiber under different nonlinearity profiles. It can be seen that pulse durations are almost identical at the front end, and they gradually become different with increased propagation distance. This indicates that even with the same values of the nonlinearity parameter at both ends, the pulse evolution is influenced by the nonlinearity profile. Pulse durations of compressed pulses are shown in Figure 2c; a sharp increase from 78 fs to 133 fs occurs as the nonlinearity profile changes from convex to concave. The reason for this is that the convex profile has a

larger nonlinearity parameter along the whole fiber, which intensifies the nonlinear effect to generate a broader spectrum. As a result, the concave profile has a higher nonlinear threshold and is more suitable for achieving high-power pulses. Figure 2c also shows M factors and SRs for different nonlinearity profiles. It can be seen that all M factors are <0.04 and SRs are >0.95. This indicates that T-YDFs with different nonlinearity profiles can output parabolic pulses with linear chirps.

Thus, we numerically demonstrate that the long T-YDF can achieve SSA with different nonlinearity parameter profiles and confirm the analytical solution. However, gain bandwidth and stimulated Raman scattering in the long fiber will cause the pulse evolution to deviate from the exact asymptotic solution, which degrades the pulse quality and limits the pulse energy [11,13]. To overcome the above challenges, short gain fibers are combined with pre-shaping technology to manage the pulse evolution, accelerating convergence towards the self-similar regime [29,30]. This approach increases the pulse energy while maintaining high pulse quality. To further verify the theoretical and numerical results and experimentally investigate the pulse evolution in the short T-YDF, we built a femtosecond self-similar amplification system based on the commercially available short T-YDF.

4. Experimental Setup

The experimental setup is shown in Figure 3. The laser source is an all-fiber femtosecond laser with an Yb-doped fiber oscillator and two-stage single-mode pre-amplifiers, delivering 300 mW pulses at 1034 nm with a 49 MHz repetition rate. The pre-shaper, which consists of a half-wave plate (HWP), a polarizing beam splitter (PBS), a 1000 lines/mm transmission grating pair and an 8 nm interference bandpass filter, can adjust the chirp, center wavelength, and energy of input pulses. By adjusting the distance of the grating pair, the chirp value of input pulses can be changed. The input pulse energy can be changed by the HWP and PBS. The central wavelength can be adjusted by changing the filter's angle relative to the beam. To confirm T-YDFs with different nonlinearity profiles can achieve SSA, two different LMA T-YDFs are used as the main amplifiers, counter-pumped by a 976 nm laser diode. The core diameter of tapered fiber 1 (TGModule A, Ampliconyx, Tampere, Finland) gradually increases from 9 μm to 40 μm over its 1.8 m length (Figure 3a). Fiber 2 (Yb-MCOF tapered fiber, INO, Québec, QC, Canada) features a 0.7 m center taper area that connects a 1.2 m long 35 μm thin end and a 0.5 m long 56 μm wide end (Figure 3b). After amplification, output pulses are compressed using a 1000 lines/mm grating pair with an efficiency of 84%.

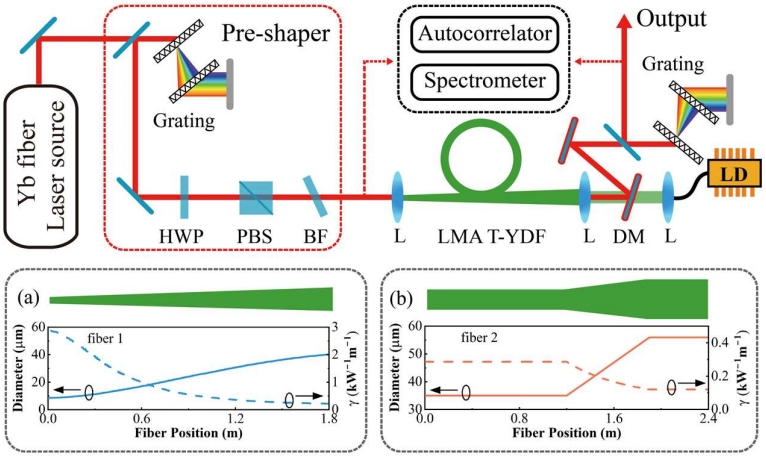

Figure 3. Schematic of experimental setup. HWP: half-wave plate; PBS: polarizing beam splitter; BF: bandpass filter; L: lens; DM: dichroic mirror; and LD: laser diode. Insets (**a**,**b**) show core diameter profiles (solid line) and nonlinearity profiles (dashed line) of fiber 1 and fiber 2, respectively.

In the experiment, the SSA is judged by the quality of the autocorrelator (AC) trace after compression due to the linear chirp being the most important characteristic of SSA [14,15]. Furthermore, the temporal intensity profile is retrieved by the phase and intensity from the correlation trace and spectrum only (PICASO) algorithm [31]. Here, the genetic algorithm is used to adjust the phase of the measured spectrum until the AC trace of the retrieved pulse and the measured AC trace are nearly identical, at which time the procedure is terminated [31]. As mentioned in Section 3, SRs of compressed pulses are calculated to evaluate the chirp and pulse quality.

5. Experimental Results and Discussion

In SSA, gain, SPM and GVD co-determine the pulse evolution. As a result, the energy and chirp of input pulses need to be adjusted to optimize the evolution to output linearly chirped pulses. Also, the gain-shaping effect influences the spectrum broadening and distorts the pulse profile. It will induce an asymmetric profile and poor quality of compressed pulses when the spectral center of the pulse and gain do not match, so the central wavelength of the input pulses needs to be adjusted by the filter [29,30].

Firstly, we explore the amplified results of two types of T-YDFs under a low pump power (20 W). As shown in Figure 4, dechirped pulses have nearly the same AC traces as TL pulses, and the SRs are both larger than 0.9, confirming the T-YDF can achieve SSA.

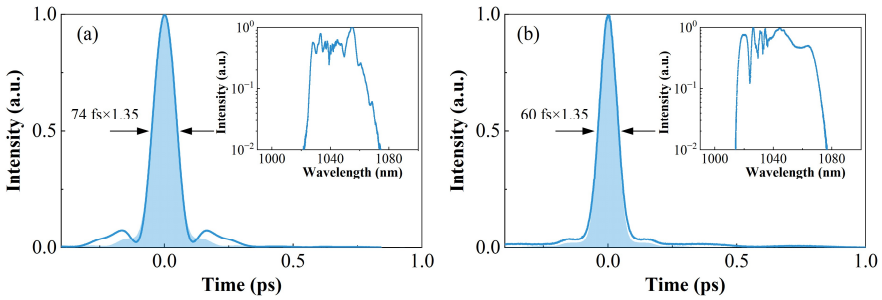

Figure 4. The AC traces of dechirped pulses (solid line) and TL pulses (shaded area) under 20 W pump power of (**a**) fiber 1 and (**b**) fiber 2. The insets show output spectra. The deconvolution factor of 1.35 is calculated from the spectrum.

Evolutions of SR and the dechirped pulse duration of fiber 1 when the pump power further increases are shown in Figure 5a. The pulse duration monotonically decreases to 46 fs until the pump power reaches 40 W. Though the SR decreases as pump power increases from 20 W to 40 W due to a narrower gain bandwidth and stronger gain-shaping effect at a higher pump power, it is remarkable that the SR is still >0.87 across the whole range, showing that SSA is achieved. Figure 5b,c show AC traces of dechirped pulses when the pump power is 30 W and 40 W for fiber 1 and fiber 2. It can be seen that obvious pedestals exist for fiber 1 and the pulse quality of fiber 2 still remains high. The reason for this is that fiber 2 has a larger core diameter at the thin end, which requires a longer distance to complete the spectral and temporal compression, thus alleviating the gain-shaping effect. This result indicates that the T-YDF with a large core diameter can achieve SSA with a high pulse quality. To further investigate SSA under high power, we focus on the pulse evolution in fiber 2.

Thus, we change pump power to explore the pulse evolution in fiber 2 under different output powers. Due to gain influencing the pulse evolution, initial chirp must be adjusted to optimize the evolution under different pump powers. The initial chirp is set to zero when input pulses are compressed to the shortest duration. Then, the change in grating spacing can adjust the value and sign of the initial chirp, which is calculated based on the center wavelength, grating spacing, groove density, and incident angle [32]. The

input power is 34 mW. Figure 6a shows evolutions of the optimal initial chirp and SR versus output power. It is obvious that the optimal initial chirp linearly decreases with the output power. The negatively chirped input pulses firstly suffer from spectral and temporal compressions due to SPM and the normal GVD in the fiber, inducing a higher peak power and narrower bandwidth when spectral and temporal compressions are finished. Spectral and temporal compressions can help alleviate the gain shaping in the front end and accelerate the evolution to SSA. The higher pump power enhances the gain shaping, so a smaller initial chirp is needed to resist the gain shaping with the scaling of output powers. Though gain shaping exists, SRs of dechirped pulses can also reach above 0.88 across the whole range of output powers, indicating a highly linear chirp of amplified pulses, a typical characteristic of SSA. The spectral bandwidth and dechirped pulse duration versus output power after optimization are shown in Figure 6b. The spectral bandwidth rapidly increases to 90 nm and pulse duration rapidly decreases to 39 fs with increasing output power, until 30 W, depending on SPM, broadens the bandwidth. However, the finite gain bandwidth resists the spectral broadening when further increasing output powers, so the spectral broadening slows down. Finally, we obtain 34 fs and 51 W average power, and the output spectrum is shown in Figure 6d. The corresponding PICASO-retrieved pulse profiles almost coincide with the TL pulse profiles, as shown in Figure 6c.

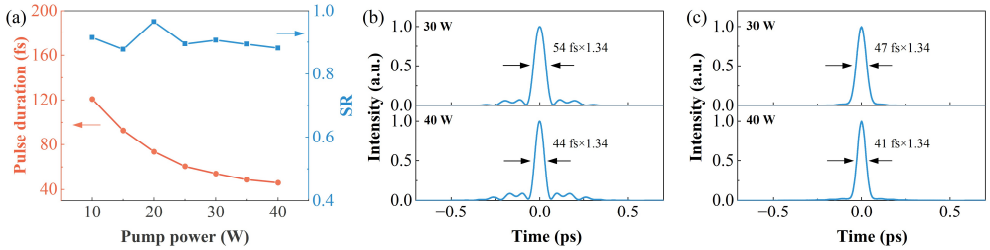

Figure 5. (**a**) Evolutions of the pulse duration and SR of dechirped pulses versus pump power for fiber 1. AC traces of compressed pulses under 30 W and 40 W pump power for (**b**) fiber 1 and (**c**) fiber 2. The deconvolution factor of 1.34 is calculated from the spectrum.

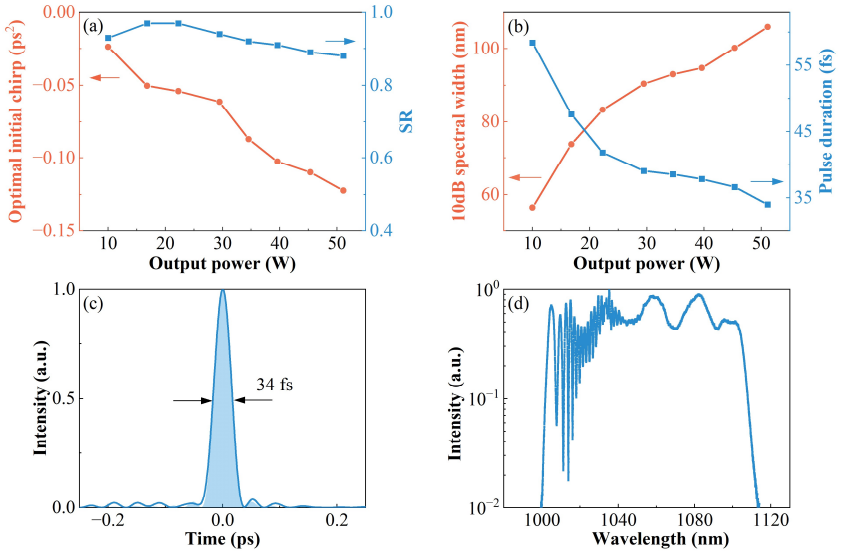

Figure 6. (**a**) Evolutions of the optimal initial chirp and SR versus the output power. (**b**) Evolutions of the spectral bandwidth and dechirped pulse duration versus the output power. (**c**) Retrieved temporal profiles (solid line), corresponding TL pulses (shaded area) and (**d**) output spectrum at 51 W output power.

6. Conclusions

In conclusion, we extend SSA to an LMA T-YDF with longitudinally decreasing nonlinearity. We transform an NLSE with a constant gain and decreasing nonlinearity into an NLSE with an equivalent gain, which previously demonstrated that an exact asymptotic solution exists, corresponding to linearly chirped parabolic pulses. Thus, the theoretical analysis indicates that T-YDFs with different nonlinearity profiles can achieve self-similar evolution. Further simulation results for five different nonlinearity profiles of T-YDFs indicate they all can generate parabolic pulses with a nearly linear chirp. To further verify the theoretical and numerical results, we built an SSA system using two kinds of T-YDFs with different nonlinearity profiles, and the results indicate they can both achieve self-similar evolution. In addition, the potential of the T-YDF to generate high-quality pulses with high power is studied, and the results indicate a proper initial negative chirp can help obtain nearly TL pulses, and the value of the optimal initial chirp decreases as the output power increases. Finally, the system can achieve self-similar evolution across a wide range of pump powers and generate 51 W average power and 34 fs nearly TL pulses with a 32 dB gain. The high-gain feature simplifies the system and helps build a compact high-power femtosecond laser source.

Currently, the core diameter of the T-YDF at the wide end can reach 97 μm and the average power can increase to 513 W with a 44 dB gain, and the thin end with a 10 μm core diameter can maintain single-mode output [33]. The high gain, high nonlinear threshold and single-mode input end are desired to achieve compact all-fiber high power femtosecond laser sources. Though the rod fiber also has a large core diameter, the length is limited to 1 m, which is too short for pulse evolution. The length of the T-YDF can be designed to be several meters, which provides a sufficient distance to evolve, and the nonuniform longitudinal profile may result in different pulse evolutions of the GMN amplification regime compared with uniform fibers [9].

Author Contributions: Conceptualization, Y.W., B.L. and M.H.; Data curation, Y.W.; Methodology, Y.W. and G.B.; Investigation, Y.W.; Funding acquisition, B.L.; Supervision, M.H.; Writing—original draft preparation, Y.W.; Writing—review and editing, Y.W., B.L. and M.H. All authors have read and agreed to the published version of the manuscript.

Funding: This research was supported by the National Natural Science Foundation of China (62435005) and the National Key Research and Development Program of China (2021YFB3602600).

Data Availability Statement: The data is contained within the article.

Conflicts of Interest: The authors declare no conflicts of interest.

References

1. Phillips, K.C.; Gandhi, H.H.; Mazur, E.; Sundaram, S.K. Ultrafast Laser Processing of Materials: A Review. *Adv. Opt. Photonics* **2015**, *7*, 684–713. [CrossRef]
2. Klas, R.; Kirsche, A.; Gebhardt, M.; Buldt, J.; Stark, H.; Hädrich, S.; Rothhardt, J.; Limpert, J. Ultra-Short-Pulse High-Average-Power Megahertz-Repetition-Rate Coherent Extreme-Ultraviolet Light Source. *PhotoniX* **2021**, *2*, 4–12. [CrossRef]
3. Maiuri, M.; Garavelli, M.; Cerullo, G. Ultrafast Spectroscopy: State of the Art and Open Challenges. *J. Am. Chem. Soc.* **2020**, *142*, 3–15. [CrossRef]
4. Sidorenko, P.; Buttolph, M.; Mejooli, M.; Eom, C.-Y.; Schaffer, C.B.; Wise, F. Evaluation of a Gain-Managed Nonlinear Fiber Amplifier for Multiphoton Microscopy. *Biomed. Opt. Express* **2023**, *14*, 2324–2332. [CrossRef]
5. Pedersen, M.E.V.; Johansen, M.M.; Olesen, A.S.; Michieletto, M.; Gaponenko, M.; Maack, M.D. 175 W Average Power from a Single-Core Rod Fiber-Based Chirped-Pulse-Amplification System. *Opt. Lett.* **2022**, *47*, 5172–5175. [CrossRef] [PubMed]
6. Su, M.; Meng, X.; Jiao, T.; Zhao, X.; Feng, S.; Tai, B.; Huang, Y.; Zhang, G.; Li, P. 134 W, 1.34 mJ, 240 fs Ultrashort Pulses from a Rod-Type Photonic Crystal Fiber Amplifier. *Opt. Lett.* **2025**, *50*, 4538–4541. [CrossRef]
7. Chen, H.-W.; Lim, J.; Huang, S.-W.; Schimpf, D.N.; Kärtner, F.X.; Chang, G. Optimization of Femtosecond Yb-Doped Fiber Amplifiers for High-Quality Pulse Compression. *Opt. Express* **2012**, *20*, 28672–28682. [CrossRef]

8. Huang, J.; He, W.; Lan, P.; Zhang, Q.; Lu, P. Generation of Sub-50 Fs, Multi-Microjoule Laser Pulses with Divided Pulse Nonlinear Amplification. *Opt. Lett.* **2025**, *50*, 5037–5040. [CrossRef] [PubMed]
9. Sidorenko, P.; Fu, W.; Wise, F. Nonlinear Ultrafast Fiber Amplifiers beyond the Gain-Narrowing Limit. *Optica* **2019**, *6*, 1328–1333. [CrossRef]
10. Fermann, M.E.; Kruglov, V.I.; Thomsen, B.C.; Dudley, J.M.; Harvey, J.D. Self-Similar Propagation and Amplification of Parabolic Pulses in Optical Fibers. *Phys. Rev. Lett.* **2000**, *84*, 6010–6013. [CrossRef] [PubMed]
11. Soh, D.B.; Nilsson, J.; Grudinin, A.B. Efficient Femtosecond Pulse Generation Using a Parabolic Amplifier Combined with a Pulse Compressor. II. Finite Gain-Bandwidth Effect. *J. Opt. Soc. Am. B* **2006**, *23*, 10–19. [CrossRef]
12. Deng, Y.; Chien, C.-Y.; Fidric, B.G.; Kafka, J.D. Generation of Sub-50 fs Pulses from a High-Power Yb-Doped Fiber Amplifier. *Opt. Lett.* **2009**, *34*, 3469–3471. [CrossRef] [PubMed]
13. Soh, D.B.; Nilsson, J.; Grudinin, A.B. Efficient Femtosecond Pulse Generation Using a Parabolic Amplifier Combined with a Pulse Compressor. I. Stimulated Raman-Scattering Effects. *J. Opt. Soc. Am. B* **2006**, *23*, 1–9. [CrossRef]
14. Zhao, J.; Li, W.; Wang, C.; Liu, Y.; Zeng, H. Pre-Chirping Management of a Self-Similar Yb-Fiber Amplifier towards 80 W Average Power with Sub-40 fs Pulse Generation. *Opt. Express* **2014**, *22*, 32214–32219. [CrossRef]
15. Liu, Y.; Li, W.; Luo, D.; Bai, D.; Wang, C.; Zeng, H. Generation of 33 Fs 935 W Average Power Pulses from a Third-Order Dispersion Managed Self-Similar Fiber Amplifier. *Opt. Express* **2016**, *24*, 10939–10945. [CrossRef]
16. Fedotov, A.; Noronen, T.; Gumenyuk, R.; Ustimchik, V.; Chamorovskii, Y.; Golant, K.; Odnoblyudov, M.; Rissanen, J.; Niemi, T.; Filippov, V. Ultra-Large Core Birefringent Yb-Doped Tapered Double Clad Fiber for High Power Amplifiers. *Opt. Express* **2018**, *26*, 6581–6592. [CrossRef]
17. Petrov, A.; Odnoblyudov, M.; Gumenyuk, R.; Minyonok, L.; Chumachenko, A.; Filippov, V. Picosecond Yb-Doped Tapered Fiber Laser System with 1.26 MW Peak Power and 200 W Average Output Power. *Sci. Rep.* **2020**, *10*, 17781. [CrossRef] [PubMed]
18. Li, W.; Ma, P.; Lai, W.; Song, J.; Wang, T.; Ren, B.; Liu, W.; Zhou, P.; Si, L. Tapered Active Fiber Simultaneously Enabled 141 W High Average and 1.3 MW High Peak Power via All-Fiber and Polarization-Maintained Picosecond Amplifier. *Opt. Laser Technol.* **2022**, *152*, 108166. [CrossRef]
19. Cao, X.; Li, Q.; Li, F.; Zhao, H.; Zhao, W.; Wang, Y.; Li, D.; Yang, Y.; Wen, W.; Si, J. Femtosecond Yb-Doped Tapered Fiber Pulse Amplifiers with Peak Power of over Hundred Megawatts. *Opt. Express* **2023**, *31*, 5507–5518. [CrossRef] [PubMed]
20. Koptev, M.Y.; Anashkina, E.A.; Bobkov, K.K.; Likhachev, M.E.; Levchenko, A.E.; Aleshkina, S.S.; Semjonov, S.L.; Denisov, A.N.; Bubnov, M.M.; Lipatov, D.S. Fibre Amplifier Based on an Ytterbium-Doped Active Tapered Fibre for the Generation of Megawatt Peak Power Ultrashort Optical Pulses. *Quantum Electron.* **2015**, *45*, 443–450. [CrossRef]
21. Fathi, H.; Motorin, E.; Aghayari, E.; Lindner, F.; Grishchenko, A.; Gribanov, E.; Wondraczek, K.; Gumenyuk, R.; Filippov, V. Yb-Doped Tapered Double-Clad Fibers with Polarization Maintenance for Half-kW Power Amplifiers. *Opt. Express* **2024**, *32*, 33064–33074. [CrossRef]
22. Wang, T.; Ren, B.; Li, C.; Guo, K.; Leng, J.; Zhou, P. Monolithic Tapered Yb-Doped Fiber Chirped Pulse Amplifier Delivering 126 μJ and 207 MW Femtosecond Laser with near Diffraction-Limited Beam Quality. *Front. Optoelectron.* **2023**, *16*, 30–39. [CrossRef] [PubMed]
23. Ren, B.; Li, C.; Wang, T.; Guo, K.; Wu, J.; Su, R.; Ma, P.; Zhou, P. Generation of Ultrafast Laser with 11 MW Peak Power from a Gain-Managed Nonlinear Tapered Fiber Amplifier. *Opt. Laser Technol.* **2023**, *160*, 109081. [CrossRef]
24. Xie, C.; Ning, T.; Zheng, J.; Pei, L.; Wang, J.; Li, J.; You, H.; Wang, C.; Gao, X. Amplification Characteristics in Active Tapered Segmented Cladding Fiber with Large Mode Area. *High Power Laser Sci. Eng.* **2021**, *9*, e32. [CrossRef]
25. Kruglov, V.I.; Peacock, A.C.; Dudley, J.M.; Harvey, J.D. Self-Similar Propagation of High-Power Parabolic Pulses in Optical Fiber Amplifiers. *Opt. Lett.* **2000**, *25*, 1753–1755. [CrossRef]
26. Shi, C.; Wang, X.; Zhou, P.; Xu, X.; Lu, Q. Theoretical Study of Mode Evolution in Active Long Tapered Multimode Fiber. *Opt. Express* **2016**, *24*, 19473–19490. [CrossRef] [PubMed]
27. Finot, C.; Parmigiani, F.; Petropoulos, P.; Richardson, D. Parabolic Pulse Evolution in Normally Dispersive Fiber Amplifiers Preceding the Similariton Formation Regime. *Opt. Express* **2006**, *14*, 3161–3170. [CrossRef]
28. Schimpf, D.; Seise, E.; Limpert, J.; Tünnermann, A. Self-Phase Modulation Compensated by Positive Dispersion in Chirped-Pulse Systems. *Opt. Express* **2009**, *17*, 4997–5007. [CrossRef]
29. Wang, S.; Chen, W.; Qin, P.; Song, Y.; Hu, M.; Liu, B. Spectral and Temporal Breathing Self-Similar Evolution in a Fiber Amplifier for Low-Noise Transform-Limited Pulse Generation. *Opt. Lett.* **2016**, *41*, 5286–5289. [CrossRef] [PubMed]
30. Song, H.; Liu, B.; Li, Y.; Song, Y.; He, H.; Chai, L.; Hu, M.; Wang, C. Practical 24-fs, 1-μJ, 1-MHz Yb-Fiber Laser Amplification System. *Opt. Express* **2017**, *25*, 7559–7566. [CrossRef] [PubMed]
31. Nicholson, J.W.; Rudolph, W. Noise Sensitivity and Accuracy of Femtosecond Pulse Retrieval by Phase and Intensity from Correlation and Spectrum Only (PICASO). *J. Opt. Soc. Am. B* **2002**, *19*, 330–339. [CrossRef]

32. Backus, S.; Durfee, C.G.; Murnane, M.M.; Kapteyn, H.C. High Power Ultrafast Lasers. *Rev. Sci. Instrum.* **1998**, *69*, 1207–1223. [CrossRef]
33. Ustimchik, V.; Chamorovskii, Y.; Filippov, V. High Average Power (500W/50ps) and High Peak Power (3.2 MW/50ps) Picosecond Pulsed MOPA System with Tapered Double-Clad Ytterbium Fiber. In *Proceedings of the Fiber Lasers XIX: Technology and Systems*; SPIE: San Francisco, CA, USA, 2022; p. 50.

Disclaimer/Publisher's Note: The statements, opinions and data contained in all publications are solely those of the individual author(s) and contributor(s) and not of MDPI and/or the editor(s). MDPI and/or the editor(s) disclaim responsibility for any injury to people or property resulting from any ideas, methods, instructions or products referred to in the content.